GUIDED-WAVE-BASED DAMAGE DETECTION OF TIMBER POLES USING A HIERARCHICAL DATA FUSION ALGORITHM

Y. Yu*
School of Civil and Environmental Engineering, University of Technology, Sydney
Sydney, NSW, 2007, Australia. yang.yu@uts.edu.au (Corresponding Author)

U. Dackermann
School of Civil and Environmental Engineering, University of Technology, Sydney
Sydney, NSW, 2007, Australia. ulrike.dackermann@uts.edu.au

J. Li
School of Civil and Environmental Engineering, University of Technology, Sydney
Sydney, NSW, 2007, Australia. jianchun.li@uts.edu.au

N. Yan
School of Civil and Environmental Engineering, University of Technology, Sydney
Sydney, NSW, 2007, Australia. ning.yan@student.uts.edu.au

ABSTRACT

This paper presents a hierarchical data fusion algorithm based on the combination of wavelet transform (WT), back propagation neural network (BPNN) and Dempster-Shafer (D-S) evidence theory for the multi-sensor guided-wave-based (GW-based) damage detection of in-situ timber utility poles. In the data-level fusion, noise elimination is performed on the original wave data to obtain single-mode signals using WT technology. Statistical information is extracted from the single-model signals as major characteristic parameters. In the feature-level fusion, for each sensor in the testing system, two sub-networks corresponding to different types of GW signals are constructed based on BPNN and characteristic parameters are sent to the networks for initial state recognition. In the decision-level fusion, the D-S evidence theory method is adopted to combine the initial results from different sensors for final decision making. The overall algorithm employs a hierarchical configuration, in which the results from the former level are regarded as input to the next level. To validate the proposed method, it was tested on GW signals from in-situ timber poles. The obtained damage detection results clearly demonstrate the effectiveness and accuracy of the proposed algorithm.

KEYWORDS

Damage detection, timber pole, data fusion, wavelet transform, neural network, evidence theory.

INTRODUCTION

Utility poles made of timber are extensively used all over the world since they are relatively low cost and environmentally friendly. Especially in Australia, timber utility poles represent a significant part of the country's infrastructure for power distribution and communication networks. There are nearly 7 million timber poles in the current network in Australia, and among them, 5 million poles are used for power and communication supply with an estimated value of more than $10 billion (Crews & Horrigan 2000). Every year, $40-$50 million is spent on maintenance and asset management to prevent utility lines from failure (Nguyen et al. 2004). The lack of reliable tools for assessing the condition of in-situ poles seriously jeopardizes the maintenance and asset management. For instance, in the Eastern States of Australia, about 300,000 electricity poles are replaced annually. However, up to 80% of them are still in a very good serviceable condition, resulting in massive waste of natural resources as well as money (Nguyen et al. 2004).

To address the requirements of the utility pole asset management industry, several non-destructive testing (NDT) GW-based methods have been developed for distinguishing healthy from unhealthy poles/piles and for identifying damage (e.g. Van et al. 1980; Dackermann et al. 2013). The principle of GW-based methods is that an impact force is initially generated and the response from the pile/pole structure is recorded by a sensor deployed on the pile/pole head. By analysing the reflective signals, predictions on the health condition can be made (Dackermann et al. 2014). Although GW methods have been used for many years for various structures including poles, the detection results still suffer from the following problems: i) Measurement sensors may be affected by background noise resulting in detection information that has great ambiguity. ii) The information obtained from one signal type is always incomplete due to its own deficiencies and environmental interference.

In view of these issues, this work proposes a reliable method with multi-source information processing for timber pole damage detection. Therefore, two different types of signals (longitudinal and bending waves) are used in the presented testing system. Furthermore, to improve the accuracy of the detection results, multi-sensors are incorporated in the system. However, since different sensors may generate conflicting detection results, due to the deployment position, it is difficult to conclude a right decision. Thus, a conflicting results combination method for reliable decision making is employed to avoid false detection results. Therefore, this work proposes a hierarchical data fusion algorithm. In different levels, different approaches are adopted to process the detection information. The effectiveness of the proposed method is validated with experimental field data. The results show that the new approach can detect the state of the poles accurately and effectively.

METHODOLOGY

The configuration of the proposed method is illustrated in Figure 1. It can be seen that the whole model adopts a hierarchical structure, in which the results from the former level are used as the inputs to the next level. Therefore, the method is able to separately realize multiple and different levels of detection information processing, which ensures the accuracy and reliability of the detection results

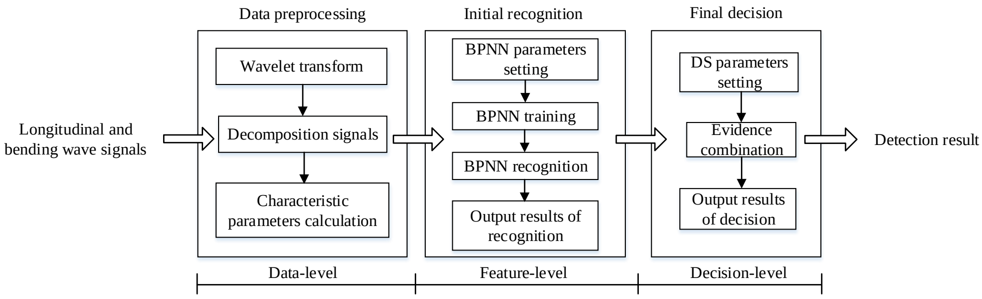

Figure 1. The hierarchical model of the proposed method

Data-level Fusion based on Wavelet Transform

In this work, the *db* wavelet is utilized for transforming the sampling signals. Generally, the larger the decomposition scale, the more favorable it is to eliminate noise. However, some important local singular characteristics may be lost if the decomposition scale is too large. In accordance with the frequency feature of the sampling signals, the maximal decomposition scale n should meet the following equation:

$$\frac{f_s}{2^{n+1}} \geq f_{\min} \tag{1}$$

where f_s denotes the sampling frequency while $f_{\min}$ denotes the lowest identification frequency.

Considering the wavelet spectra and different characteristics in each scale, an appropriate threshold is chosen by a heuristic approach. For the points whose values are smaller than the threshold, their coefficients are set as 0; otherwise their coefficients are set as the differences between points' values and the threshold. In this way, the single mode signals without noise are acquired.

Feature-level Fusion based on Neural Network

In accordance with the requirement for timber pole damage detection, the number of network output nodes is 2. The aim vector (0, 1) means the pole state is 'healthy', while (1, 0) denotes the unhealthy pole. Six statistical characteristics, such as mean value, mean amplitude, variance, skewness and peak frequency, are extracted from the longitudinal wave signals as the input vector to build the sub-BPNN 1. Eight parameters of mean amplitude, peak frequency, probability density, and energy distribution factors in four frequency bands are extracted from the bending wave signals as the input vector to constitute sub-BPNN 2. For the design of the hidden layer, an empirical equation is adopted to determine the neuron number of the hidden layer, shown as (Wang et al. 2005):

$$n_h = \sqrt{p+q} + \beta \tag{2}$$

where p and q denote the neuron numbers in input and output layers, respectively. β is a constant between 1 and 10.

Then the heuristic BP algorithm is employed to adjust the learning rate in the course of training. Weight and bias are able to be updated by the following equations:

$$\begin{aligned} \Delta W^d(k) &= \gamma \Delta W^d(k-1) - (1-\gamma) a s^d (a^{d-1})^T \\ \Delta b^d(k) &= \gamma \Delta b^d(k-1)(1-\gamma) a s^d \end{aligned} \tag{3}$$

where γ=0.95 denotes the momentum factor; a is the learning rate; $W^d(k)$, $b^d(k)$ and s^d denote the weight vector, bias vector and sensitivity function in level d.

Decision-level Fusion based on D-S Evidence Theory

Based on the practical application of timber pole damage detection, the decision process can be described as follows:
The frame of discernment of pole damage detection is $\theta = \{A_1, A_2\}$. A_1 denotes the unhealthy state while A_2 denotes the healthy state. Suppose $Y_i(j)$ (j=1,2,3) is the output vector of BPNN i (i=1,2), and α_i denotes the detection reliability coefficient of sub BPNN i. In this paper, the empirical values of α_1 and α_2 are 0.89 and 0.91 by a great deal of simulation trials.

In the first-layer evidence combination, outputs of BPNN 1 and BPNN 2 are regarded as the evidence of discernment frame after data normalization. The basic probability assignment (BPA) of evidence i is given as:

$$\begin{cases} m_i^1(A_j) = \dfrac{\alpha_i Y_i(j)}{\sum_{j=1}^{q} Y_i(j)} \\ m_i^1(\Theta) = 1 - \alpha_i \end{cases} \tag{4}$$

where $Y_i(j)$ denotes the j^{th} output of BPNN i. After finishing the first-layer combination, the results are regarded as the BPAs in the second-layer combination. Through multi-layer evidence combination, the detection results can be effectively improved and the difficulty of decision making avoided. The combination rule of evidences A and B can be written as (Si et al. 2014):

$$\begin{cases} m_{1\oplus 2}(A) = 0, \qquad A = \varnothing \\ m_{1\oplus 2}(A) = \dfrac{\sum_{A_i \cap A_j = A} m_1(A_i) m_2(B_j)}{1-K}, \quad K = \sum_{A_i \cap A_j = \varnothing} m_1(A_i) m_2(B_j) \end{cases} \tag{5}$$

where m_1 and m_2, respectively, denote the BPAs in the same discernment frame, focal elements of which are A_i and B_j. K denotes the conflict weight.

In accordance with the evidence combination results from Eq. 5, the maximum trust degree approach is used to make the final decision:

$\exists A_1, A_2 \subset \theta$, $m(A_1)=\max\{m(A_k), A_k \subset \theta\}$ and $m(A_1)=\max\{m(A_k), A_k \subset \theta$ and $A_k \neq A_1\}$. If the following relationship is satisfied:

$$\begin{cases} m(A_1) - m(A_2) > \varepsilon_1 \\ m(\Theta) < \varepsilon_2 \\ m(A_1) < m(\Theta) \end{cases} \tag{6}$$

A_1 is the decision result, where ε_1 and ε_2 are thresholds. In this work, ε_1=0.1 and ε_2=0.05.

EXPERIMENTAL RESULTS AND ANALYSIS

The experimental setup is illustrated in Figure 2 (a) and (b). An impact hammer is adopted to generate the GWs and seven sensors are used to measure the wave response signals. The hammer impact is induced at a height of 1.8 m in either longitudinal direction to generate the longitudinal waves (LW) or transverse direction to generate bending waves (BW). The responses are captured by seven piezoresistive sensors which are installed in a line 0.2 m off ground with 0.2 m spacing between the sensors. The signal acquisition and analysis is conducted with NI software Labview. For each experiment, the sampling frequency is 1 MHz with a testing duration of 0.5 s, thus 500,000 sampling data are obtained in each test. Two types of tests are conducted, i.e. longitudinal and transverse tests. For longitudinal testing, the impact is induced in the longitudinal direction with an impact angle and the sensors are set to measure acceleration in the vertical direction. For transverse testing, the impact is executed vertical to the poles and the sensors capture acceleration in the horizon direction. For each type, five tests are carried out. Therefore, a total of 70 sampling signals are obtained for each pole. After the testing, the poles were cut into several sections to determine their states: healthy or unhealthy. An example of the post mortem autopsy of one of the poles is shown in Figure 2 (c).

(a) (b) (c)

Figure 2. Testing and autopsy of timber poles.
(a) Experimental testing, (b) field testing and (c) post mortem autopsy results.

Figure 3 shows the LW signals of an unhealthy pole from the seven sensors. It is obvious that the original sampling signal is mixed with a great deal of noise and other interferences; thus, it is difficult to distinguish the damage feature from these signals. To further analyze the signals without noise, wavelet transform technology is utilized to divide the original signals into three levels. The transformed results of a LW signal from sensor 1 are shown in Figure 4. It can be seen that the signal of the third level is relatively smoother and steadier than the original signal. Moreover, this signal contains most energy of the original signal. Consequently, the low frequency signal in the third level is taken as the single-mode signal to extract the damage information.

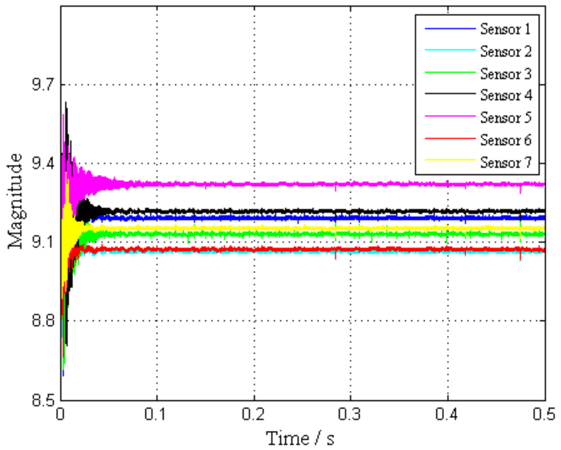

Figure 3. Original signals of LW

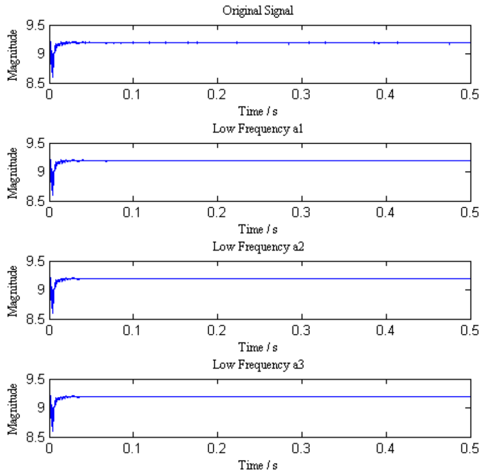

Figure 4. LW Signal decomposition of sensor 1

Next, the characteristic parameters mentioned in the Methodology Section are calculated from the single-mode signals. A total of 50 samples are selected to train sub-BPNN 1 and sub-BPNN 2. In this work, the neural network toolbox v8.0 (Matlab v.2012bm the Mathworks, Inc.) is employed to set up the network models. The NN parameters are set as follows: training accuracy e=0.01, learning rate le=0.9. Log-sigmoid function and tan-sigmoid function are selected as transfer functions in the hidden and output layers, respectively. According to the empirical equation, the neuron numbers of the hidden layer in the two sub-BPNNs are all in the range of [5, 14]. Table 1 shows the resulting training times and false accept rate (FAR) of the two BPNNs for the different hidden layer neuron numbers (5 to 14). It can be seen that the optimal structure of BPNN 1 is (6,7,2), while the optimal structure of BPNN 2 is (8,10,2). In this case, the networks have faster convergence as well as higher recognition accuracy.

Table 1. Training times and FAR for different neuron numbers

Neuron numbers in hidden layer	BPNN 1		BPNN 2	
	Training times	FAR	Training times	FAR
5	2.53 x 10^4	10%	4.72 x 10^4	10%
6	3.74 x10^4	10%	3.67 x 10^4	15%
7	0.93 x 10^4	5%	3.29 x 10^4	5%
8	4.89 x 10^4	20%	1.84 x 10^4	10%
9	1.36 x 10^4	15%	2.78 x 10^4	15%
10	2.11 x 10^4	10%	1.23 x 10^4	5%
11	1.73 x 10^4	5%	1.94 x 10^4	10%
12	0.78 x 10^4	15%	2.37 x 10^4	10%
13	0.97 x 10^4	15%	2.71 x 10^4	5%
14	1.82 x 10^4	10%	3.82 x 10^4	15%

In order to evaluate the effectiveness of the algorithm, a healthy pole is selected as the testing sample for method validation. Table 2 shows the BPA functions after initial recognition by the neural network. It is clearly seen from Table 2 that the detection results of sensors 2 and 5 disagree with the practical state. The main reason contributing to this phenomenon is that the training sample number is so limited that it does not comprise all situations, leading to recognition errors in the detection result. Table 3 displays the first-layer combination results of BPNN 1 and BPNN 2 while Table 4 shows the combination results of all seven sensors. It can be seen from Table 3 that after the first-layer combination, the support probability of A_2 (healthy) of sensor 1 ascends to 0.9185 and the support probability of A_1 (unhealthy) decreases to 0.0632 at sensor 1. However, because of $m_2(A_1)>m_2(A_2)$ and $m_5(A_1)>m_5(A_2)$, the detection results from sensors 2 and 5 are still in contradiction with the other five sensors. Therefore, it is difficult to make the final decision. Table 4 shows the second-layer combination results of all seven sensors. It is clear that after the second-layer combination, the support probability of A_2 increases to 1 while both the support probabilities of A_2 and the uncertainty decline to 0. According to Eq. 6, the final detection result is A_2 (healthy).

Table 2. Initial recognition by BPNNs

BPA	A_1	A_2	Θ
$m_{1,1}$	0.1331	0.7569	0.1100
$m_{1,2}$	0.2559	0.6541	0.0900
$m_{2,1}$	0.4648	0.4252	0.1100
$m_{2,2}$	0.5264	0.3836	0.0900
$m_{3,1}$	0.1074	0.7826	0.1100
$m_{3,2}$	0.2289	0.6811	0.0900
$m_{4,1}$	0.1561	0.7339	0.1100
$m_{4,2}$	0.2070	0.7030	0.0900
$m_{5,1}$	0.6101	0.2799	0.1100
$m_{5,2}$	0.3663	0.5437	0.0900
$m_{6,1}$	0.0617	0.8283	0.1100
$m_{6,2}$	0.1238	0.7862	0.0900
$m_{7,1}$	0.0533	0.8367	0.1100
$m_{7,2}$	0.0939	0.8161	0.0900

Table 3. First-layer combination

BPA	A_1	A_2	Θ
m_1	0.0632	0.9185	0.0183
m_2	0.5858	0.3905	0.0237
m_3	0.0433	0.9393	0.0174
m_4	0.0579	0.9244	0.0177
m_5	0.5796	0.3947	0.0257
m_6	0.0114	0.9738	0.0148
m_7	0.0072	0.9787	0.0071

Table 4. Second-layer combination

BPA	A_1	A_2	Θ
m	0	1	0

CONCLUSIONS

In this paper, a novel damage detection approach for timber utility poles is presented based on a multi-sensor testing and hierarchical decision making model. Firstly, for each sensor, wavelet transform technology is applied to the original signals to remove noise disturbances, obtaining single-mode signals and characteristic parameters. Secondly, two sub-BPNN models corresponding to each sensor are constructed for initial recognition of the pole state. Finally, on the basis of these initial results, D-S evidence combination is employed for the final decision making. Two types of GW signals are used to validate the effectiveness of the proposed method. Experimental results show that the hierarchical approach is able to considerably enhance the accuracy of the pole damage detection (the focal degree of the right proposition has increased from 0.8367 to 1). The new method overcomes the problem of difficult decision making and satisfies the requirement of damage detection of timber utility poles. In future research, it is envisaged to extend this technique to also identify the locations, severities and types of damage.

REFERENCES

Crews, K.I. and Horrigan, A. (2000) "Strength assessment of timber utility poles in Australia", *New Zealand Timber Design Journal*, Vol. 9, No. 2.

Dackermann, U., Crews, K., Kasal, B., et al. (2013) "In situ assessment of structural timber using stress-wave measurements", *Materials and Structures*, Vol. 47, No. 5, pp. 787-803.

Dackermann, U., Skinner, B. and Li, J. (2014) "Guided wave–based condition assessment of in situ timber utility poles using machine learning algorithms", *Structural Health Monitoring*, 1475921714521269.

Nguyen, M., Foliente, G. and Wang, X. (2004) "State of the practice and challenges in Non-destructive evaluation of utility poles in service", *Key Engineering Materials*, 270-273.

Si, L., Wang, Z., Tan, C., et al. (2014) "A novel approach for coal seam terrain prediction through information fusion of improved D-S evidence theory and neural network", Measurement, Vol. 54, pp. 140-151.

Van, K.H. and Middendorp, P. (1980) "Interpretation of results from integrity tests and dynamic load tests", *Proceedings, International Seminar on the Application of Stress Wave Theory in Piles*, Stockholm, Sweden, 217-232, 1980.

Wang, H.B., Xu, W.Y. and Xu, R.C. (2005) "Slope stability evaluation using back propagation neural network", *Engineering Geology*, Vol. 80, No. 3-4, pp. 302-315.